Article

Frequency-Based Flood Risk Assessment and Mapping of a Densely Populated Kano City in Sub-Saharan Africa Using MOVE Framework

Ali Aldrees [1], Abdulrasheed Mohammed [2], Salisu Dan'azumi [1,2,*] and Sani Isah Abba [3]

1 Department of Civil Engineering, College of Engineering in Al-Kharj, Prince Sattam bin Abdulaziz University, Al-Kharj 11942, Saudi Arabia; a.aldrees@psau.edu.sa
2 Department of Civil Engineering, Faculty of Engineering, Bayero University Kano, Kano 700241, Nigeria; abdulrasheeddoko@gmail.com
3 Interdisciplinary Research Center for Membranes and Water Security, King Fahd University of Petroleum and Minerals, Dhahran 31261, Saudi Arabia; sani.abba@kfupm.edu.sa
* Correspondence: sdanazumi.civ@buk.edu.ng; Tel.: +966-597138132

Abstract: Flooding is a major environmental problem facing urban cities, causing varying degrees of damage to properties and disruption to socio-economic activities. Nigeria is the most populous African country and Kano metropolis is the second largest urban center in Nigeria, and the most populated in Northern Nigeria. The aim of the paper was to conduct a flood risk assessment of Kano metropolis. The city is divided into two hydrological basins: the Challawa and Jakara basins. Flood frequency analyses for 2 to 100-year return periods were carried out for both the basins using a Log-Pearson Type III distribution and flood inundation and hazard mapping was carried out. The social vulnerability to flooding of both basins was assessed using the method for the improvement of vulnerability assessment in Europe (MOVE) framework. Flood risk was determined as a product of flood hazard and flood vulnerability. The results showed that areas of 50.91 and 40.56 km^2 were vulnerable to a 100-year flood. The flood risk map for the two basins showed that 10.50 km^2 and 14.23 km^2 of land in Challawa and Jakara basins, respectively, was affected by the risk of a 100-year flood, out of which 11.48 km^2 covers built-up areas. As the city is densely populated, with a population density of well over 20,000 persons per square kilometer in the highly built-up locations, this means that much more than 230,000 persons will be affected by the flood risk in the two basins.

Keywords: flood hazard; social vulnerability; flood risk; flood mapping; kano metropolis

1. Introduction

In recent years, climate change and the rapid urbanization of cities have caused significant urban flooding resulting in traffic disturbances, the disruption of services, damage to properties and critical infrastructure, harm to vulnerable populations, and sometimes the loss of lives [1–3]. An important contribution to threats posed by floods is the generation of flood maps and the estimation of flood risk [4]. Generally, "risk" is defined as the potential consequences of a hazard and flood maps indicate the inundated areas based on the rising water levels, although flood maps alone are not adequate to assess risks to property, infrastructure, and services due to flood events. Therefore, socio-economic factors are critical for a flood risk assessment [5]. The United Nations International Strategy for Disaster Reduction (UNISDR) [6] defined a risk assessment as a process or application of a methodology for evaluating risk as defined by the geographic coverage of the hazard, the exposure of people, property, and infrastructure to the hazard, and the vulnerability of people, property, and infrastructure to the event. A flood risk assessment is a systematic procedure to identify, analyze, and quantify the real and expected damage threats of flooding [7].

A flood hazard is a potentially damaging phenomenon which may cause loss of life or injury, property damage, social and economic disruption, and environmental degradation [8]. Flood hazards have increased in recent years due to climate change, fast socio-economic development, population growth, and the inefficient use of land. An urban flood hazard assessment is important for the mitigation of floods and a necessary step for government policies on urban planning worldwide [4]. They help the planners manage better the sites for urban development and recognize areas that probably need stormwater runoff infrastructure [8]. Flood hazards have increased in recent years because of different factors, such as climate change, subsidence, fast socio-economic development, population growth, the inefficient use of land, and urbanization, resulting in an increased amount of impervious surfaces [9,10]. Generally, flood hazard assessment and mapping are used to identify areas at risk of flooding, and, consequently, to improve flood risk management. The assessments and maps typically look at the expected extent and depth of flooding corresponding to various return periods [11]. In the context of Kano city, Temitope [12] generated a unit hydrograph for the River Jakara in Kano metropolis using rainfall data. Abaje et al. [13] investigated the changing rainfall pattern in Kano over a period of 6 decades. Mohammed et al. [14] examined rainfall dynamics and climate change in Kano using 100 years of rainfall data and Mohammed et al. [15] examined the gaps between climate change and urbanization in Kano city.

According to the Intergovernmental Panel on Climate Change [16], vulnerability is defined as "the degree to which a system is susceptible to, and unable to cope with, adverse effects of climate change, including climate variability and extremes". Vulnerability determines how people will be affected and where they are spatially located [17]. Vulnerability is a multi-faceted concept with varying characteristics or dimensions in nature. It is a set of multiple stressors that act together to determine the vulnerability of an area. These stressors include the geographical location, the exposure of the population and infrastructure, the socio-economic and cultural conditions, the political and institutional structures, and the coping and adaptive capacity that differentiate the impacts on people and the human system [18]. This also means that an area may be highly exposed to a hazard such as a flood, but be less vulnerable if it has adequate means to adapt to the flood. Vulnerability is therefore not only a matter of exposure, but rather a combination of exposure with local socio-economic factors [18]. Flanagan et al. [19] argued that social vulnerability refers to the socio-economic and demographic factors that affect the resilience of communities. Social vulnerability can have multiple forms: it can be the state of the system before the event, the likelihood of outcomes in terms of economic losses and life lost, and the lack of capacities or weaknesses to face and recover quickly when the disaster strikes. A better understanding of the level of vulnerability and how the susceptible population is distributed can be beneficial for the better management of flood risk [20]. There are numerous studies that have considered the vulnerabilities of social, economic, and environmental systems to flooding [21–25]. Action Aid [26] investigated the vulnerability of six African cities on the basis of key management criteria including local people's perceptions of the causes of flooding, adaptation, and the community's social coping capacity. Nabegu [24] assessed the vulnerability of households in the study area to a flood disaster, using a questionnaire survey, infrastructure analysis and flood impact information. Social vulnerability refers to the characteristics of a person or group in terms of their capacity to anticipate, cope with, resist, and recover from the impact of a natural hazard [27]. Social vulnerability is related to gender, class, race, age, poverty, and many more factors [28]. In this study, social vulnerability was considered because the study area was an urban center with a significant population and valuable assets.

There are a number of multi-criteria evaluation concepts that are being used in assessing social vulnerability such as the Analytical Hierarchy Process [29,30] and the method for the improvement of vulnerability in Europe (MOVE) framework [18]. In the MOVE framework, a characterization of vulnerability is performed through three key factors, namely, (1) exposure, (2) susceptibility, and (3) lack of resilience [18]. The MOVE framework was

developed as a vulnerability assessment framework, arising from the MOVE project carried out from 2008 to 2011 in Europe. It was developed based on past vulnerability projects in Europe, but the concept is used worldwide [27]. The advantages of the MOVE framework is that it can be applied to assess vulnerability not only to floods, but other natural disasters such as droughts, extreme temperature, earthquakes, etc. It can be used to analyze physical, social, economic, social, environmental, cultural, and institutional vulnerabilities at different geographical scales. Lianxiao and Morimoto [27] used the MOVE framework and the Information Entropy Method to carry out a spatial analysis of social vulnerability to floods in Katsushika Ward, Tokyo, Japan. Williams and Muhammad [31] applied the MOVE framework with ArcGIS 10.2 to assess social vulnerability to malaria in Katsina-Ala, Benue State, Nigeria. Kablan et al. [18] used the MOVE framework to assess social vulnerability to floods in urban Côte d'Ivoire and Sane et al. [32] applied the MOVE framework to assess social vulnerability to floods in Medina Gounass Dakar, Senegal. Even though the MOVE framework was developed in Europe [33,34], it is applied worldwide including in Pakistan [35], Japan [27], and Africa [18,32]. The MOVE framework was also used by researchers to assess the level of vulnerability due to climate change impacts [36,37].

Other approaches, such as machine learning, have been used by researchers in urban flood risk assessments. Choubin et al. [38] used model averaging, classification and regression trees, and support vector machine to develop a machine learning model that can be used for flood hazard assessment based on return periods. Variables used as the input include precipitation, elevation, distance from stream, slope, land use, flow accumulation, drainage density, topographic wetness index, soil order, normalized difference vegetation index, flow accumulation, aspect, curvature, and lithology. Sentinel 1 Radar images were used to identify flooded images with different return periods for model validation. The results showed that the models performed very well, with an accuracy greater than 90%. Taromideh et al. [39] integrated the multi-criteria decision-making technique of the analytic hierarchy process and machine learning techniques of classification and regression models to develop an urban flood risk map. The results showed that the urban flood hazard was mostly influenced by drainage density, and the distance to the river and to vulnerable areas. Likewise, urban flood vulnerability was mostly influenced by land use, dwelling quality, population density, household income, and the distance to hospitals and cultural heritage centers. The flood risk map classified the areas into five categories, going from very low to very high flood risk areas. Many researchers have integrated either decision-making approaches with machine learning or big data analytic techniques in conjunction with GIS to model the flood hazard and/or vulnerability [40–46].

No study known to the researchers has integrated a frequency-based flood hazard assessment with the multi-criteria evaluation method of the MOVE framework. The lack of such a study on flood hazard estimation for the whole city makes it difficult to determine the possible areas that are prone to flooding with a view to propose mitigation measures. The present study is the first to use flood frequency analysis to estimate the flood hazard and then integrate the flood hazard with flood vulnerability assessments to determine the flood risk in a densely populated sub-Saharan African city.

2. Materials and Methods

A framework showing flow chart of the methodology used in carrying out this research is presented as Figure 1.

2.1. The Study Area

Kano metropolis is located in north-western Nigeria. The city's nucleus is located at latitude 11.75° N and longitude 12.52° E. The metropolis covers total area of 499 km^2 with a total population of approximately 3,931,300 inhabitants (as projected from the last 2006 Census figure). It is the second largest industrial center in Nigeria and the most populous city in Northern Nigeria. The population density of Kano city is well over 20,000 per square kilometer [15]. The city experiences a mean annual rainfall of approximately 800 mm, with

wet season occurring mainly from June to September. Great temporal variation occurs in the amount of rainfall received and no two consecutive years record the same amount [14]. Figure 2 shows the administrative map of Kano metropolis. The city is drained by two river basins: Challawa and Jakara.
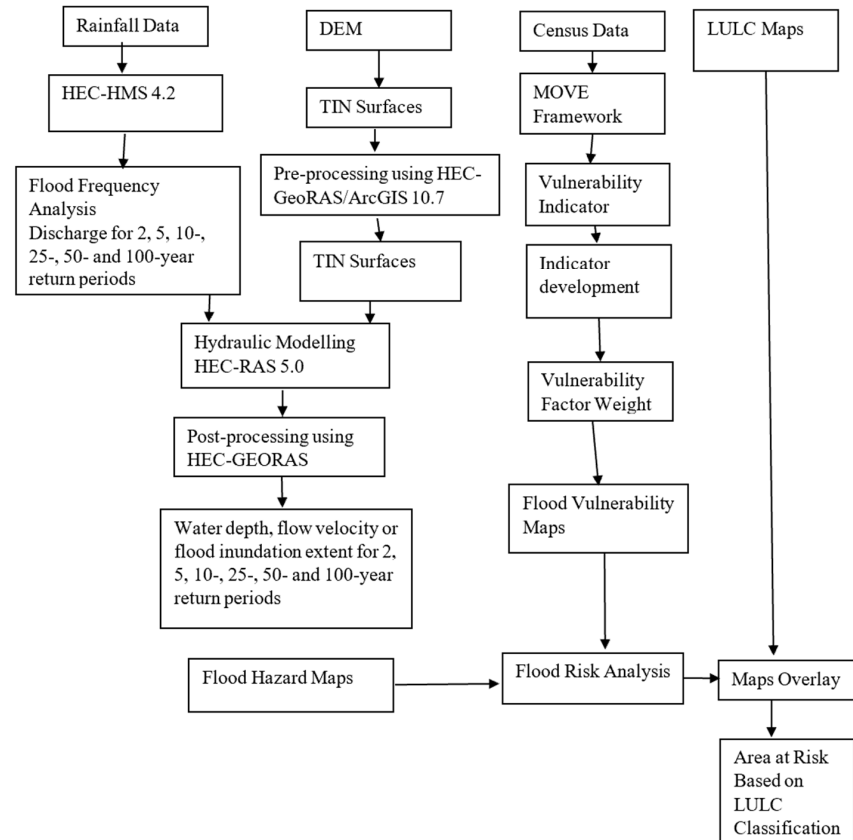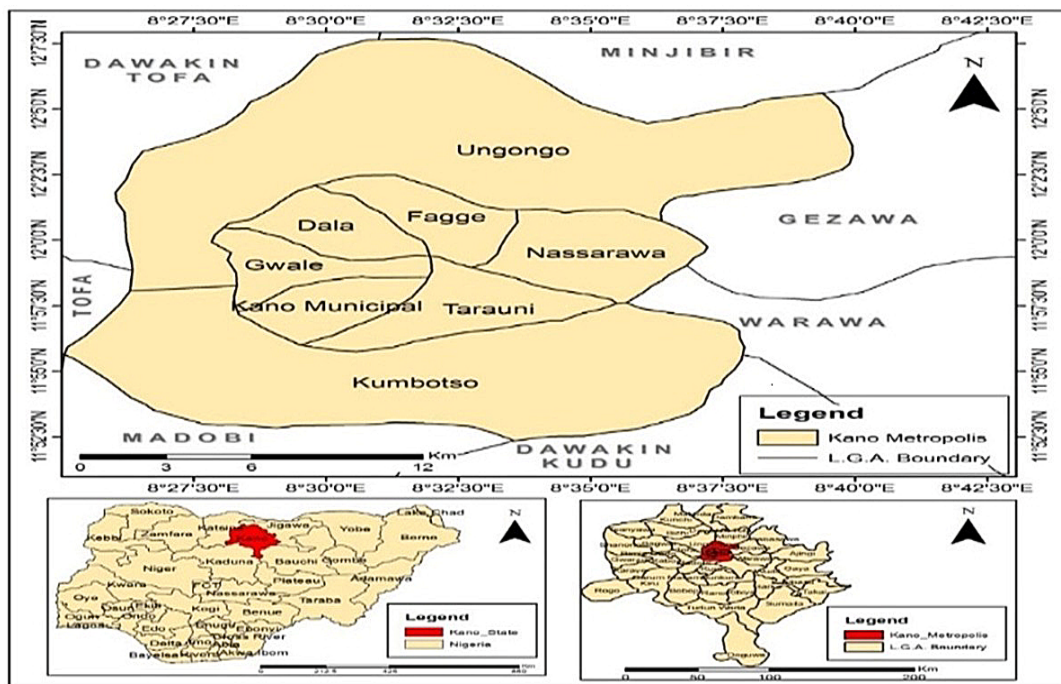

Figure 1. Flowchart of methodology.

Figure 2. Map of Kano metropolis.

2.2. Determination of Flood Hazard

The hydrology of Kano city is divided into two main basins, the Challawa and Jakara basins, which serve as main receptacles of runoff from the city. Challawa was delineated into (15) sub-basins with a total drainage area of 105 km^2, whereas Jakara basin was delineated into (17) sub-basins with a total drainage area of 110 km^2 using Archydro tool and HEC-GeoHMS extensions in ArcGIS 10.7. Daily rainfall data for the study area were collected and streamflow for the two basins was generated using HEC-HMS rainfall–runoff transformation [39]. Goodness-of-fit test was carried on the flow data using Easyfit 5.0 and Log-Pearson Type III distribution was found to fit well. The flood frequency analysis and the corresponding flood inundation and hazard assessments were carried out for 2, 5, 10, 50, and 100-years floods using HEC-GeoRAS extension in ArcGIS 10.7 and hydraulic modelling in HEC-RAS 5.0. Flood hazard was classified using water depth and flood velocity as presented in accordance with Table 1 [47–49]. For example, a moderate-sized person begins to lose stability in 0.9 m deep water flowing at 0.6 m/s. Deep inundation and high velocity of flood are classified as destructive, while deep inundation with low velocity is classified as less destructive [50].

Table 1. Hazard as a function of flood water depth and velocity in accordance with [47].

Hazard Classification	Flood Depth (m)	Flood Velocity (m/s)
High	>1.4	>2
Medium	1–1.4	1–2
Low	0–1	0–1

2.3. Determination of Social Vulnerability

Population figures from the immediate past census year (2006) were obtained from the National Population Commission and were projected using Equation (1).

$$P = P_o e^{rt} \tag{1}$$

where P and P_o = future and current population, r = growth rate and t = time in years.

The population density was obtained using Equation (2).

$$P_d = \frac{P}{A} \tag{2}$$

where P = number of people and A = land area.

Social vulnerability to flooding was carried out using MOVE framework [51]. Characterization of vulnerability was performed through three key factors, namely, (1) exposure, (2) susceptibility, and (3) lack of resilience. These indicators are presented in Table 2.

Table 2. Indicators selected for social vulnerability assessment in accordance with [18].

Components	Symbol	Indicator	Explanation	Functional Relationship
Exposure	E1	Population density	The higher the population, the higher the exposure.	+
	E2	Elevation	The lower the elevation, the higher the exposure.	+
	E4	Inundated areas	The larger the flood inundated areas, the more exposed.	+
Susceptibility	S1	Children under 5	Fragile health and difficulty for evacuation process.	+
	S2	Elderly above 60	Fragile health and difficulty for evacuation process.	+
	S3	Disable people	Difficulty for evacuation process.	+
	S4	Women	The higher the number, the higher the susceptibility of affected people.	+

Table 2. *Cont.*

Components	Symbol	Indicator	Explanation	Functional Relationship
Resilience	LoR1	Literacy	The higher the rate, the higher the capacity to understand early warning systems.	−
	LoR2	Unemployment	Jobless people have difficulties to recover from flood damages.	+
	LoR3	Poverty	The higher the poverty rate, the difficult it is to recover from flood damage	+

Note: "+" = increasing vulnerability and "−" = decreasing vulnerability.

The indicators were first normalized using the Min–Max method in order to have values between 0 and 1. The normalized value of the indicators was computed using either Equation (3) or Equation (4) [32]. When the indicators were related positively with the vulnerability, the normalized values of the indicator were computed using Equation (3):

$$X_{ij} = \frac{x_{ij} - Min(x_{ij})}{Max(x_{ij}) - Min(x_{ij})} \quad (3)$$

When the indicators were related negatively with the vulnerability, the normalized values of the indicator were computed using Equation (4):

$$X_{ij} = \frac{Max(x_{ij}) - (x_{ij})}{Max(x_{ij}) - Min(x_{ij})} \quad (4)$$

where X_{ij} is the normalized value of indicator i of component j; x_{ij}, is the value of indicator i; and $max(x_{ij})$ and $min(x_{ij})$ are the maximum and minimum values of the indicators i of the component j, respectively.

The weights to the individual indicator (w_j) were assigned using a weighting method developed in [52], reported in [18], and presented as Equation (5):

$$w_j = \frac{c}{\sqrt{Var(x_{ij})}} \quad (5)$$

where c is the normalized constant given by Equation (6):

$$c = \left[\sum_{j=1}^{j=k} \frac{1}{\sqrt{Var(x_{ij})}} \right]^{-1} \quad (6)$$

The normalized indicators were aggregated using Equation (7):

$$(E, \ S, \ LoR) = \sum_{j=1}^{k} w_j x_{ij} \quad (7)$$

where w $(0 < w < 1)$ and $\sum_{j=1}^{k} w_j$ are the weights. Finally, the three components, that is, E, S, and LoR, were aggregated into final composite indicator of social vulnerability using Equation (8) [32].

$$V = \frac{\sum_{j=1}^{k} w_j x_j}{m} \quad (8)$$

where V = vulnerability index, m = number of components, w_j = weights for domain j, and x_j = index of component J (E, S, LoR). Therefore, the vulnerability weights were assigned for each category with 1 as the maximum in each case (Please see Supplementary Files, Table S1a–e).

The results of social vulnerability index were saved in ArcGIS 10.7 and joined with flood inundation polygon for each scenario using the Join tool in ArcGIS 10.7. The Conversion tool was then used to produce raster maps of social vulnerability category. The vulnerability maps were reclassified with vulnerability weights estimated using Reclassify spatial analysts tool in ArcGIS 10.7, and, finally, the reclassified vulnerability maps were then integrated to produce the final flood vulnerability map for each scenario. This was achieved using the Weighted sum tool in ArGIS 10.7. The maps were classified into five urban flood vulnerability classes as presented in Table 3.

Table 3. Urban flood vulnerability classification in accordance with [53].

Index Value	Classification
<0.01	Very small vulnerability to floods
0.01–0.25	Small vulnerability to floods
0.25–0.5	Vulnerability to floods
0.50–0.75	High vulnerability to floods
0.75–1	Very high vulnerability to floods

2.4. Determination of Flood Risk

The flood risk map was produced as a product of hazard map and vulnerability map using raster calculation in Map algebra spatial analyst tool in ArcGIS 10.7. The flood risk map for each scenario was produced and classified into four risk zones as High, Moderate, Low, and No risk (Table 4).

Table 4. Flood risk classification in accordance with [54].

Risk Index	Risk Classification
>4	High
2–4	Moderate
0.2–1.99	Low
0	No risk

3. Results

3.1. Flood Hazard

Tables 5 and 6 show the Challawa and Jakara catchment areas' flood hazard classification for different return periods. It can be seen that for the Challawa basin, a 2-year flood covers a total area of 9.71 km^2, while a 100-year flood covers a total area of 12.13 km^2. Likewise, a 2-year flood covers a total area of 14.35 km^2, while a 100-year flood covers a total area of 17.35 km^2 for Jakara basin. A low hazard covered the majority of the floodplain.

Table 5. Challawa basin flood hazard classification.

Hazard Class	2-Year	5-Year	10-Year	25-Year	50-Year	100-Year
Low hazard (km^2)	4.20	4.31	4.33	4.36	4.39	4.43
Medium hazard (km^2)	2.66	2.70	2.71	3.37	3.96	4.48
High hazard (km^2)	2.85	3.01	3.07	3.14	3.18	3.22
Total	9.71	10.02	10.11	10.87	11.53	12.13

Table 6. Jakara basin flood hazard classification.

Hazard	2-Year	5-Year	10-Year	25-Year	50-Year	100-Year
Low hazard (km^2)	7.14	7.66	7.83	8.14	8.28	8.50
Medium hazard (km^2)	4.12	4.11	4.16	4.06	4.07	3.97
High hazard (km^2)	3.08	3.55	3.86	4.27	4.59	4.89
Total	14.35	15.31	15.85	16.47	16.94	17.36

The maps of the flood hazard for 100-year return periods produced for Challawa and Jakara basins are shown in Figures 3 and 4 according to the classifications earlier described in Table 1. However, for all the return periods, the high hazard areas are located along the channel, but Jakara catchment is more prone to flooding than Challawa due to the higher land cover.
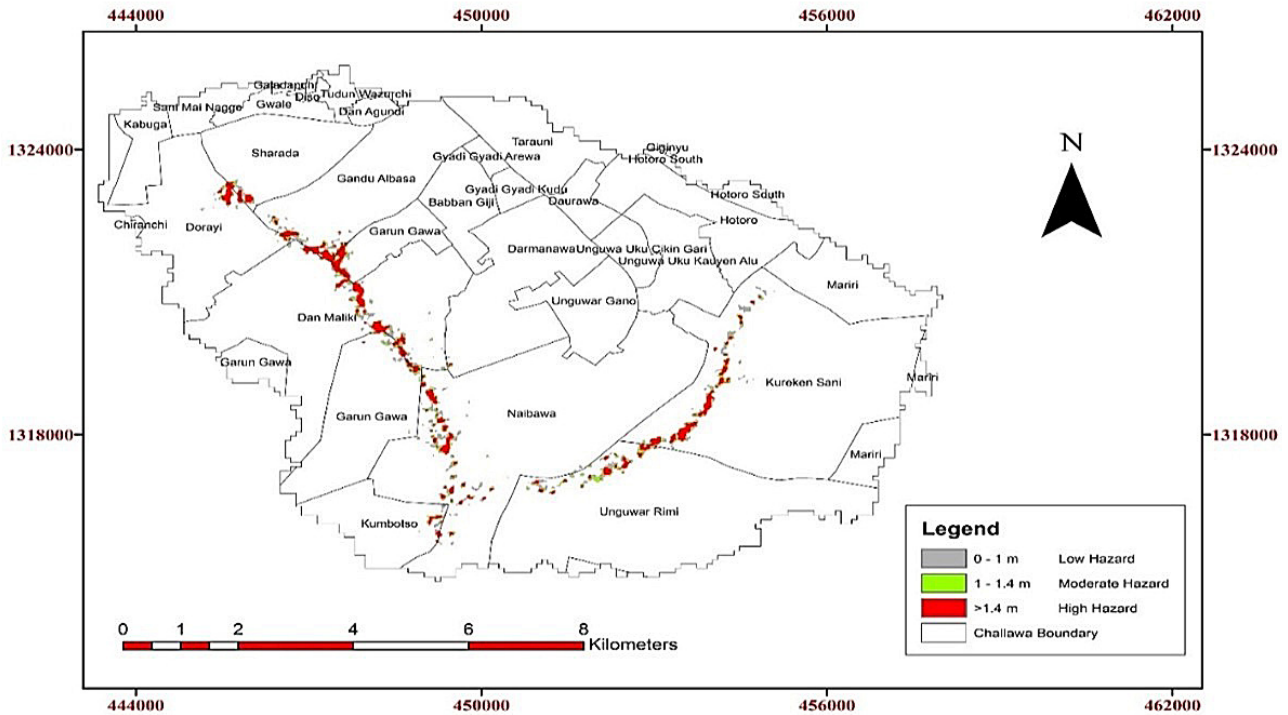

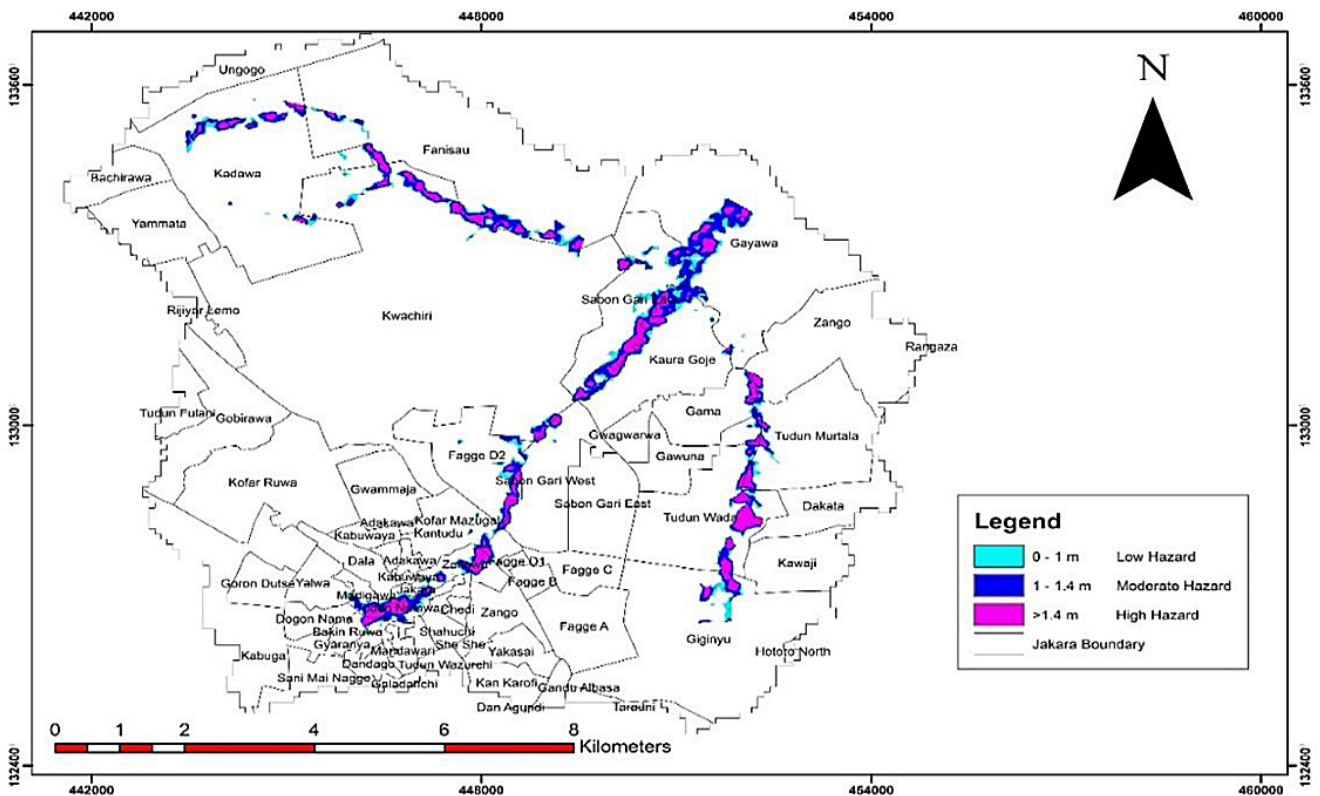**Figure 3.** 100-year flood hazard map for Challawa basin.

Figure 4. 100-year flood hazard map for Jakara basin.

3.2. Flood Vulnerability

The flood vulnerability maps of 100, 50, 25, 10, 5, and 2-year floods were obtained for Challawa basin, but only the 100-year return period is shown in Figure 5.
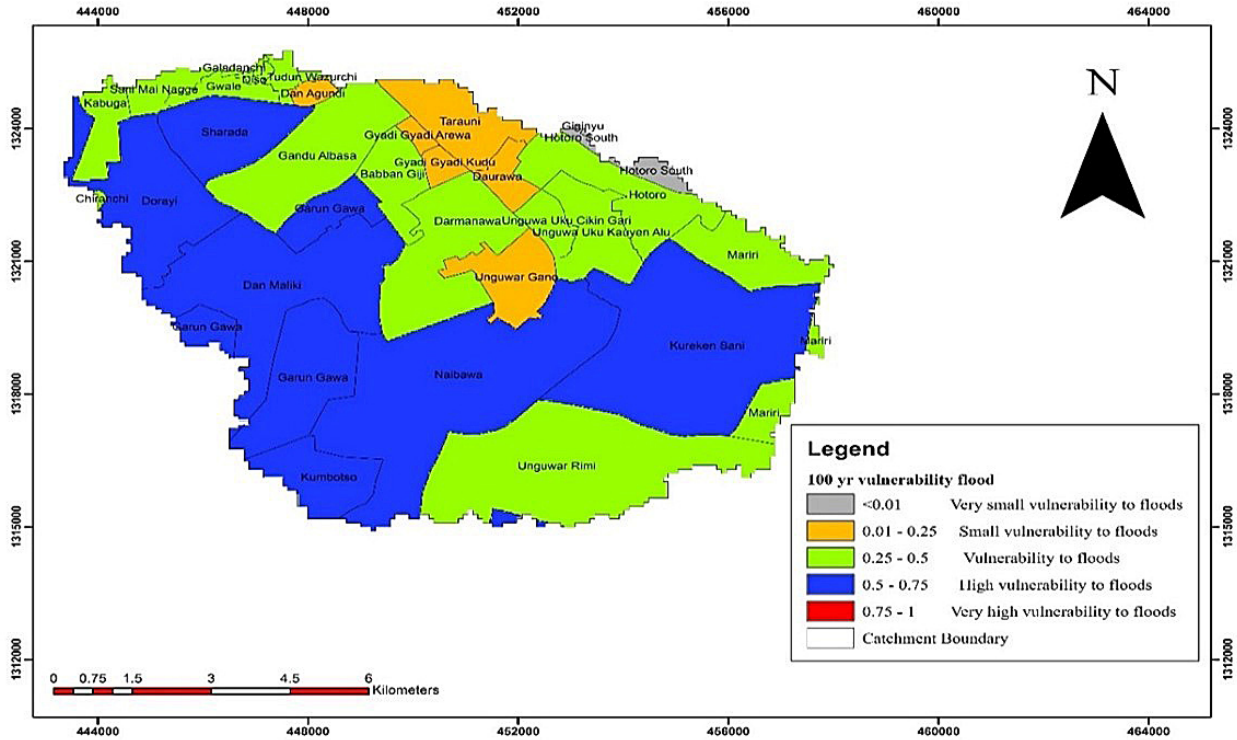

Figure 5. 100-year flood vulnerability map for Challawa basin.

From the 100-year flood vulnerability map, the wards with a high vulnerability to floods (HVF) are mainly in Kumbotso Local Government Area of Kano State. The wards that fall within the class of having a small vulnerability to floods (SVF) are in Municipal and Tarauni Local Government Area, while the remaining wards are classified as having a moderate vulnerability to floods (MVF) and there are no wards that are classified as having a very high vulnerability to floods (VHVF). Carefully examining the remaining flood scenarios, that is, the 50, 25, 10, 5, and 2-years flood vulnerability maps, it can be observed that the majority of the areas fall within the class of MVF.

Detailed flood vulnerability classifications for Challawa basin corresponding to 100, 50, 25, 10, 5, and 2-year floods are presented in Table 7. It can be observed that the vulnerability extent and severity increase with an increase in the return period. MVF areas covered an area which ranges between 19.37 and 41.23 km^2 for 100 to 2-year return periods, whereas HVF areas covered an area of 27.53 to 0 km^2 for 100 to 2-year return periods. There was no area classified as VHVF for all the scenarios considered.

Table 7. Flood vulnerability extent for Challawa basin.

Return Period	Vulnerability Class Extent (km^2)					Total
	VSVF	SVF	MVF	HVF	VHVF	
100	0.34	3.67	19.37	27.53	0	50.91
50	0.32	3.60	34.42	11.56	0	49.90
25	0.32	3.60	37.79	8.19	0	49.90
10	0.32	4.23	38.87	6.48	0	49.90
5	0.32	8.18	34.92	6.48	0	49.90
2	0.32	8.34	41.23	0	0	49.90

Notes: VSVF = very small vulnerability to floods, SVF = small vulnerability to floods, MVF = moderate vulnerability to floods, HVF = high vulnerability to floods, VHVF = very high vulnerability to floods.

Figure 6 shows the 100-year flood vulnerability map for Jakara basin. It is observed that areas that fall in the region of HVF included some parts of Municipal and Fagge Local Government Areas while the areas classified as SVF included some parts of Gwale, as well as Municipal and Fagge Local Government Areas. Observing the remaining flood scenarios, that is, 50, 25, 10, 5, and 2-year flood vulnerability maps, it can be observed that the majority of the remaining areas fall within the class of MVF. Detailed Jakara flood vulnerability classifications and the extent of each class for the 100, 50, 25, 10, 5, and 2-year return periods are presented in Table 8.
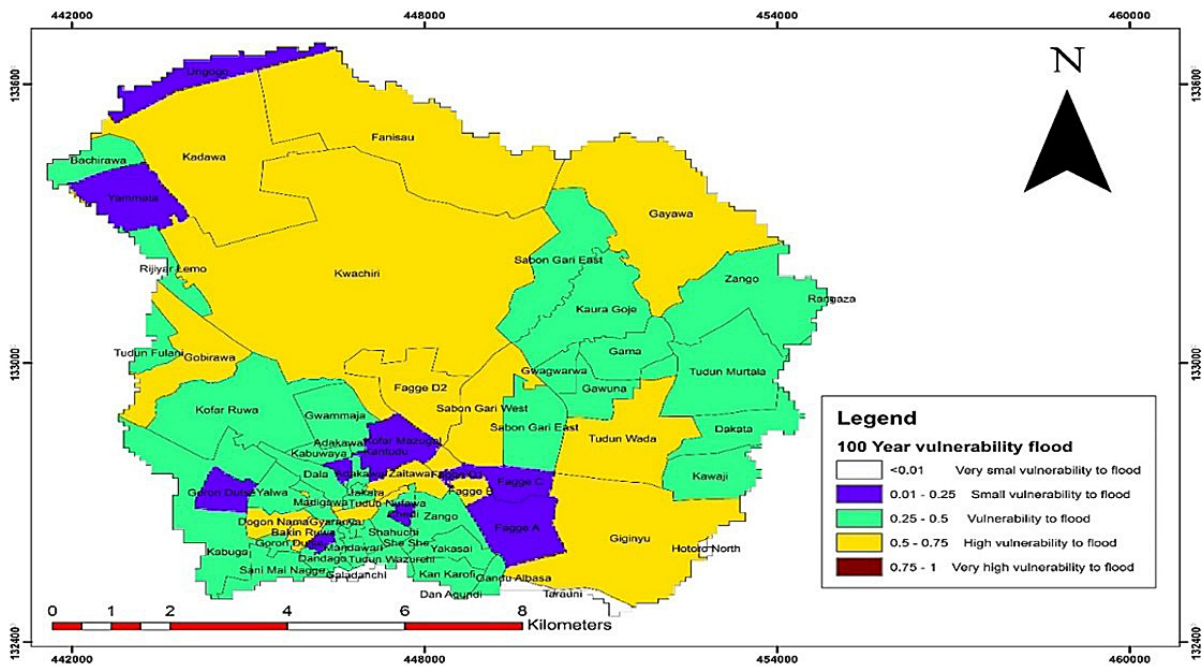

Figure 6. 100-year flood vulnerability map for Jakara basin.

Table 8. Flood vulnerability extent for Jakara basin.

Return Period	Vulnerability Class Extent (km^2)					Total
	VSVF	**SVF**	**MVF**	**HVF**	**VHVF**	
100	0.23	3.04	14.43	22.86	0	40.56
50	0.23	3.13	17.31	19.89	0	40.56
25	0.23	5.36	17.82	17.15	0	40.56
10	0.23	8.50	30.16	1.67	0	40.56
5	0.23	9.96	29.48	0.89	0	40.56
2	0.23	11.54	28.79	0	0	40.56

Table 8 shows the flood vulnerability information for Jakara basin. It can be seen that VSVF covered 0.23 km^2 for all the return periods. MVF regions covered an area of 14.43, 17.31, 17.82, 30.16, 29.48, and 28.79 km^2 for 100, 50, 25, 10, 5, and 2-year return periods, respectively. The HVF regions covered an area of 22.86, 19.89, 17.15, 1.67, 0.89, and 0 km^2 for the 100, 50, 25, 10, 5, and 2-year return periods, respectively. There was no VHVF region for all the return periods. The MOVE framework used in this research has provided information on the areas that need most intervention and factors that need to be given attention to effectively reduce the existing susceptibility and increase the resilience to flood exposure.

3.3. Flood Risk

The area covered by each flood risk category for all the return periods is presented in Table 9 for Challawa basin. The table shows that the area affected by floods also increases as

the return period increases. For a 2-year flood, low, medium, and high-risk floods covered an area of 4.44, 2.57, and 0.55 km^2, respectively, while for a 100-year flood, low, medium, and high-risk areas covered 5.43, 3.85 and 1.22 km^2, respectively. It can be observed that a large percentage of the area affected by floods is mainly of low and moderate risk levels. The high flood risk zones are mostly areas lying along the channels.

Table 9. Area covered by each risk classification for Challawa basin.

Risk Class	Return Period (Year)					
	2	5	10	25	50	100
Low Risk (km^2)	4.44	4.66	4.67	5.47	5.48	5.43
Medium Risk (km^2)	2.57	2.43	2.66	3.36	3.47	3.85
High Risk (km^2)	0.55	0.70	0.81	0.96	1.17	1.22
Total (km^2)	7.56	7.79	8.14	9.79	10.12	10.50

Maps of the flood risk were also obtained, but only that of the 100-year flood is presented in Figure 7. It can be observed that Challawa basin has two main categories of risk zones (moderate and low risk zones) for all the return periods, while the high risk zones in the catchment are very small.
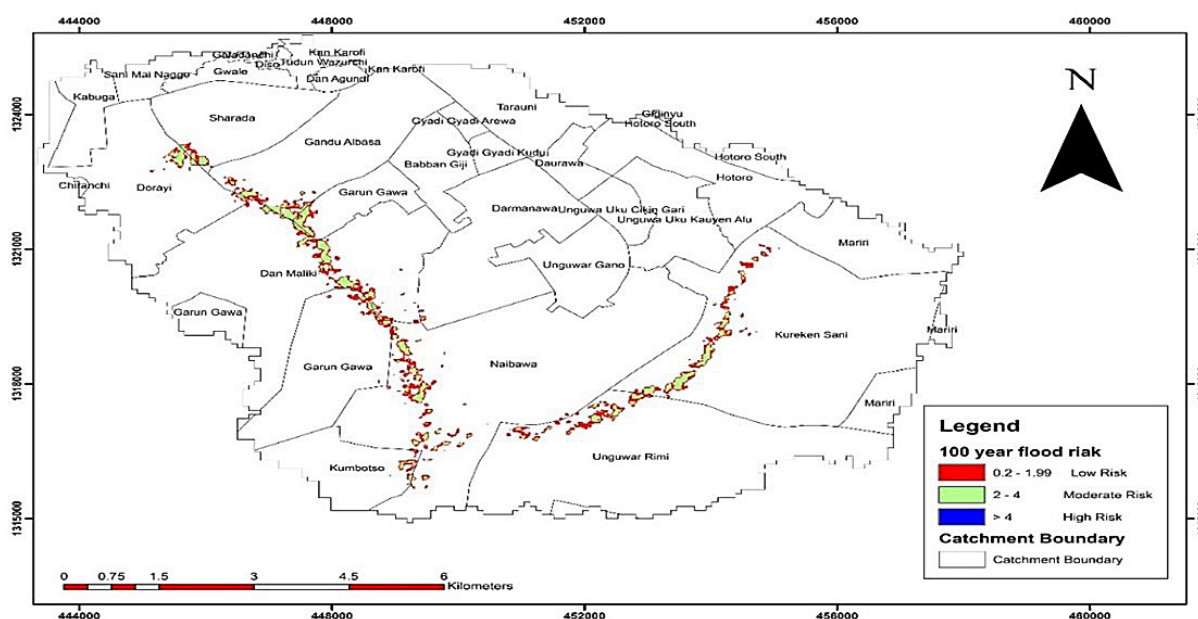

Figure 7. 100-year flood risk map for Challawa basin.

Table 10 shows the elements, based on the LULC classification, at risk of flooding. It can be observed that the LULC area at risk from a 2-year flood is 3.99, 2.66, 0.88, and 0.03 km^2 of built-up area, bare-land, vegetation, and water body, respectively. Likewise, the LULC area at risk from a 100-year flood is 4.98, 3.88, 1.54 and 0.10 km^2 of built-up area, bare-land, vegetation, and water body, respectively.

Table 10. Areal coverage of LULC at risk of flooding for Challawa basin.

LULC	Return Period (Year)					
	2	5	10	25	50	100
Built up area (km^2)	3.99	4.07	4.11	4.73	4.87	4.98
Bare land (km^2)	2.66	2.76	2.84	3.65	3.79	3.88
Vegetation (km^2)	0.88	0.90	1.12	1.32	1.36	1.54
Water body (km^2)	0.03	0.06	0.06	0.07	0.09	0.10
Total	7.55	7.79	8.13	9.78	10.11	10.50

Table 11 shows the area covered by each flood risk category for Jakara basin. A 2-year flood caused low, medium, and high risk in an area of 5.60, 3.73, and 1.04 km^2, respectively, while a 100-year flood with low, medium and high risk covered areas of 7.76, 5.17, and 1.30 km^2, respectively. It is also observed that a large percentage of the area affected by the floods was mainly of low and moderate risks. The high flood risk zones were mostly infrastructure built along the channels.

Table 11. Area covered by flood risk classification for Jakara basin.

Risk Class	Return Period (Year)					
	2	5	10	25	50	100
Low Risk (km^2)	5.60	5.71	6.75	7.07	7.61	7.76
Medium Risk (km^2)	3.73	4.59	4.74	4.96	5.02	5.17
High Risk (km^2)	1.04	1.01	1.08	1.11	1.17	1.30
Total	10.37	11.31	12.57	13.14	13.80	14.23

The maps of Jakara flood risks were obtained, but only that of the 100-year flood is presented in Figure 8. It can be seen that Jakara basin had similar flood risk zones to Challawa basin. Table 12 also shows the elements, based on the LULC classification, at risk of flooding for Jakara basin. It could be observed that the LULC are at risk from a 2-year flood are 4.17, 3.75, 1.87, and 0.09 km^2 of built-up area, bare-land, vegetation, and water body, respectively. Likewise, the LULC area at risk from a 100-year flood are 6.50, 4.85, 2.70, and 0.17 km^2 of built-up area, bare-land, vegetation, and water body, respectively. The built-up area made up the highest land cover class at risk of flooding, followed by bare land. This is due to the urban nature of the basin with considerable infrastructure in place such as residential buildings, roads, schools, hospitals, etc. This agrees with the findings of [55], which attributed the flood in Kano to an increased LULC area. As the city's population density is well over 20,000 persons per square kilometer in the highly built-up locations, this means that much more than 100,000 and 130,000 persons will be affected by the flood risk in the Challawa and Jakara basins, respectively.
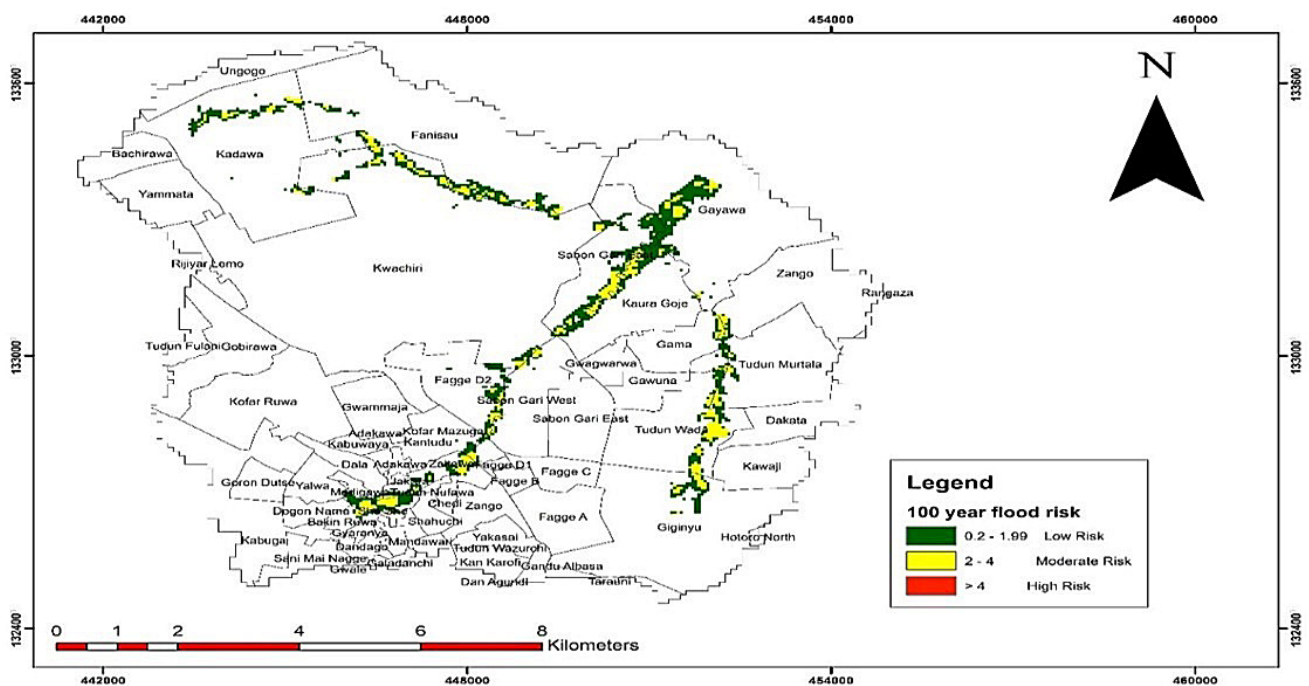

Figure 8. Jakara flood risk map for 100-year return period.

Table 12. Areal coverage of LULC at risk of flooding for Jakara basin.

LULC	Return Period (Year)					
	2	5	10	25	50	100
Built-up area (km^2)	4.67	5.18	5.59	5.87	6.28	6.50
Bare land (km^2)	3.75	3.93	4.45	4.58	4.69	4.85
Vegetation (km^2)	1.87	2.09	2.42	2.56	2.65	2.70
Water body (km^2)	0.09	0.10	0.11	0.14	0.17	0.17
Total	10.38	11.30	12.57	13.15	13.79	14.23

4. Discussion

Flooding has been a major source of concern arising from the huge economic losses encountered. The type of flood in Kano is pluvial and usually occurs annually during the rainy season, affecting mainly the urban areas in Nigeria. Such floods, which are arguably unprecedented in recent times, are caused by more frequent and severe rainfall which overwhelms the capacity of drainage systems. Nkwunonwo [23] reported that flooding occurs annually during the rainy season between July and October, ravaging many cities in Nigeria. Presently, the occurrence of such floods due to poor urban planning is an important issue in flood risk mitigation. The pluvial flooding occurs when rainfall–runoff, which ought to be evacuated by the drainage system, remains on impermeable surfaces and flows overland or into local depressions and topographically low areas to create temporary ponds. It mostly occurs after a short, intense downpour which cannot be evacuated quickly enough by the drainage system or seep into the ground [56]. Built environments generate higher surface runoff, in excess of the local drainage capacity, thereby causing local floods [10,57]. Intense urbanization, rapid conversion of green spaces to residential and commercial areas, and neglect to town-planning and landscape conservation have resulted in the emergence of urban slums in the city, which has further aggravated the flood risk [58].

Climate change impacts are also known to have a severe impact on the urban drainage system. Climate change increases the intensity of rainfall events posing a major threat to stormwater infrastructure systems [59]. Higher rainfall intensities lead to more severe storms, with expected increases in damage to urban centers. Pluvial flooding has been predicted to become more frequent due to climate change and urbanization [60]. Kano city is extremely overcrowded, which constantly threatens the city's infrastructural management systems. Due to the population size, the sewage and waste water management system is overburdened, the drainage network system is inadequate, and there are cases of dumping of household and commercial refuse in open landfills and direct discharges to the streams and drains. The integration of urban growth and climate change scenarios into flood risk management models as proposed by researchers [61,62] could go a long way in addressing flood issues in developing countries. In the absence of climate change prediction models, flood hazard mapping using flood frequency estimates coupled with flood vulnerability can serve as viable tools to address flood problems in developing countries. However, it is worth noting that the flood plain areas studied are urban catchments which have long been inhabited with densely populated settlements. There is no agency, whether governmental or non-governmental, that keeps a record of floods during the storm events in the basins. Therefore, no field data were available to validate the flood hazard results with observed data, as the two catchments are ungauged.

5. Conclusions

A flood frequency analysis for 2, 5, 10, 25, 50, and 100-year return periods was carried out using the Log Pearson Type III distribution and flood hazard and inundation mappings for Challawa and Jakara basins of Kano metropolis were developed. For the 100-year return period flood, a total area of 12.13 km^2 would be inundated for Challawa basin while a total area of 17.36 km^2 would be inundated for Jakara basin. Generally, for both catchment areas, it can be concluded that most of the flood hazard areas fall within the category of

low and medium hazards, but high hazard areas were also located along the channels, and districts that are prone to flooding were identified. Social vulnerability was assessed and the districts that fell within the categories of VSVF, SVF, HVF, MVF, and SVF were identified and classified for return periods of 2 to 100-year floods. A total area of 50.91 and 40.56 km^2 was found to be affected by the different categories of vulnerabilities for the 100-year flood, but there was no VHVF zone for all the return periods considered. A flood risk map for the two basins was developed, and 10.50 km^2 of land was affected by the risk of a 100-year flood, of which 4.98 km^2 is built-up area in Challawa basin. For Jakara basin, 14.23 km^2 of land area was affected, of which 6.50 km^2 is a built-up area. As the city is densely populated, with a population density of well over 20,000 persons per square kilometer in the highly built-up locations, this means that much more than 230,000 persons will be affected by flood risk in the two basins.

References

1. Rangari, V.A.; Umamahesh, N.V.; Patel, A.K. Flood-hazard risk classification and mapping for urban catchment under different climate change scenarios: A case study of Hyderabad city. *Urban Clim.* **2021**, *36*, 100793. [CrossRef]
2. Yiyi, H.; Stephan, T.; Paolo, A.; Jun, R. Flood impacts on urban transit and accessibility—A case study of Kinshasa. *Transp. Res. Part D Transp. Environ.* **2021**, *96*, 102889. [CrossRef]
3. Adegun, O.B. Flood-related challenges and impacts within coastal informal settlements: A case from Lagos, Nigeria. *Int. J. Urban Sustain. Dev.* **2023**, *15*, 1–13. [CrossRef]
4. Cai, S.; Fan, J.; Yang, W. Flooding risk assessment and analysis based on GIS and the TEN-AHP method: A Case Study of Chongqing Chaina. *Atmosphere* **2021**, *12*, 623. [CrossRef]
5. Armenakis, C.; Du, E.X.; Natesan, S.; Persad, R.A.; Zhang, Y. Flood Risk Assessment in Urban Areas Based on Spatial Analytics and Social Factors. *Geosciences* **2017**, *7*, 123. [CrossRef]
6. UNISDR (United Nations International Strategy for Disaster Reduction). *UNISDR Terminology on Disaster Risk Reduction*; UNISDR: Geneva, Switzerland, 2015; p. 30.
7. Zhang, X.; Yi, L.; Zhao, D. Community-based disaster management: A review of progress in China. *Nat. Hazards* **2013**, *65*, 2215–2239. [CrossRef]
8. Bathrellos, G.D.; Karymbalis, E.; Skilodimou1, H.D.; Gaki-Papanastassioul, K.; Baltas, E.A. Urban flood hazard assessment in the Basin of Athens Metropolitan City, Greece. *Environ. Earth Sci.* **2016**, *75*, 319. [CrossRef]
9. Bruijn, K.M.; Klijn, F.; Van de Pas, B.; Slager, C.T.J. Flood fatality hazard and flood damage hazard: Combining multiple hazard characteristics into meaningful maps for spatial planning. *Nat. Hazards Earth Syst. Sci.* **2015**, *15*, 1297–1309. [CrossRef]
10. Aldrees, A.; Dan'azumi, S. Application of Analytical Probabilistic Models in Urban Runoff Control Systems' Planning and Design: A Review. *Water* **2023**, *15*, 1640. [CrossRef]
11. UN Environment–DHI Center; CTCN; UNEP. Flood Hazard Assessment and Mapping; A Practitioner's Guide to Adaptation Technologies for Increased Water Sector Resilience Climate Change Adaptation Technologies for Water. 2021. Available online: https://unepdhi.org/publications/ (accessed on 9 November 2021).
12. Temitope, E.O. Generation of Unit Hydrograph for River Jakara in Kano Metropolis. Master's Thesis, Department of Civil Engineering, Bayero University Kano, Kano, Nigeria, 2010.

13. Abaje, I.B.; Ndabula, C.; Garba, A.H. Is the Changing Rainfall patterns of Kano State and its Adverse Impacts an Indication of Climate Change? *Eur. Sci. J.* **2014**, *10*, 7857–7881.

14. Mohammed, M.U.; Abdulhamid, A.; Badamasi, M.M.; Ahmed, M. Rainfall Dynamics and Climate Change in Kano, Nigeria. *J. Sci. Res. Rep.* **2015**, *7*, 386–395. [CrossRef]

15. Mohammed, M.U.; Hassan, N.I.; Badamasi, M.M. In search of missing links: Urbanization and climate change in Kano Metropolis, Nigeria. *Intern. J. Urban Sustain. Dev.* **2019**, *11*, 309–318. [CrossRef]

16. IPCC (Intergovernmental Panel on Climate Change). *Climate Change Impacts, Adaptation and Vulnerability, Contribution of Working Group II to the Fourth Assessment Report*; Report, Summary for Policy Makers; Cambridge University Press: Cambridge, UK, 2014.

17. Okayo, J.; Odera, P.; Omuterema, S. Socio-economic characteristics of the community that determine ability to uptake precautionary measures to mitigate flood disaster in Kano Plains, Kisumu County, Kenya. *Geoenviron. Disasters* **2015**, *2*, 26. [CrossRef]

18. Kablan, M.K.A.; Dango, K.; Coulibaly, M. Assessment of social vulnerability to flood in Urban Cote d'Ivoire using the MOVE frame work. *Water* **2017**, *9*, 292. [CrossRef]

19. Flanagan, B.E.; Gregory, E.W.; Hallisey, E.J.; Heitgerd, J.L.; Lewis, B. A Social Vulnerability Index for Disaster Management. *J. Homel. Secur. Emerg. Manag.* **2011**, *8*, 1–22. [CrossRef]

20. Rahman, M.A. *Social Vulnerability to Flood: An Integrated Spatial Assessment in the United States*; Association of American Geographers: Washington, DC, USA, 2018.

21. Ajibade, I.; McBean, G.; Bezner-kerr, R. Urban flooding in Lagos, Nigeria: Patterns of vulnerability and resilience among Women. *Glob. Environ. Chang.* **2014**, *23*, 1714–1725. [CrossRef]

22. Akukwe, T.I.; Ogbodo, C. Spatial Analysis of Vulnerability to Flooding in Port Harcourt Metropolis, Nigeria. *SAGE Open* **2015**, *5*, 1–19. [CrossRef]

23. Nkwunonwo, U.C.; Whitwork, M.; Baily, B. Relevance of social vulnerability assessment to flood risk reduction in the Lagos Metropolis of Nigeria. *J. Appl. Sci. Technol.* **2016**, *8*, 366–382.

24. Nabegu, A.B. Analysis of vulnerability to flood disaster in Kano State. *Greener J. Phys. Sci.* **2014**, *4*, 22–29.

25. Olajuyigbe, A.E.; Rotowa, O.O.; Durajaye, E. An assessment of flood hazard in Nigeria; the case of Mile 12, Lagos. *Mediterr. J. Soc. Sci.* **2012**, *3*, 367–375.

26. Action Aid. *Climate Change, Urban Flooding and the Rights of Urban Poor in Africa. Key Findings from Six African Cities*; Action Aid International: London, UK, 2006.

27. Lianxiao; Morimoto, T. Spatial Analysis of Social Vulnerability to Floods Based on the MOVE Framework and Information Entropy Method: Case Study of Katsushika Ward, Tokyo. *Sustainability* **2019**, *11*, 529. [CrossRef]

28. Younus, M.; Kabir, M. Climate change vulnerability assessment and adaptation of Bangladesh: Mechanisms, Notions and Solutions. *Sustainability* **2018**, *10*, 4286. [CrossRef]

29. Musungu, K.; Motala, S.; Smit, J. Using Multi-criteria evaluation and GIS for flood risk analysis in informal settlements of Cape Town: The case of Graveyard Pond. *S. Afr. J. Geomat.* **2012**, *1*, 77–91.

30. Shuaibu, A.; Hounkpè, J.; Bossa, Y.A.; Kalin, R.M. Flood Risk Assessment and Mapping in the Hadejia River Basin, Nigeria, Using Hydro-Geomorphic Approach and Multi-Criterion Decision-Making Method. *Water* **2022**, *14*, 3709. [CrossRef]

31. Williams, H.T.; Muhammed, B.U. Modelling social vulnerability to malaria risk in Katsina-Ala Local Government Area, floods, Benue State Nigeria. *J. Geogr. Environ. Earth Sci.* **2018**, *14*, 2454–57352.

32. Sane, O.D.; Gaye, A.T.; Diakhate, M.; Aziadekey, M. Social vulnerability assessment to flood in Medina Gounass Dakar. *J. Geogr. Inf. Syst.* **2015**, *7*, 415–429. [CrossRef]

33. Welle, T.; Depietri, Y.; Angignard, M.; Birkmann, J.; Renaud, F.; Greiving, S. Vulnerability Assessment to Heat Waves, Floods, and Earthquakes Using the MOVE Framework: Test Case Cologne, Germany. In *Assessment of Vulnerability to Natural Hazards*; Elsevier: Amsterdam, The Netherlands, 2014; pp. 91–124. ISBN 9780124105287. [CrossRef]

34. Jamshed, A.; Rana, I.A.; Birkmann, J.; McMillan, J.M.; Kienberger, S. A bibliometric and systematic review of the Methods for the Improvement of Vulnerability Assessment in Europe framework: A guide for the development of further multi-hazard holistic framework. *JAMBA* **2023**, *15*, 1486. [CrossRef] [PubMed]

35. Hamidi, A.R.; Wang, J.; Guo, S.; Zeng, J. Flood vulnerability assessment using MOVE framework: A case study of the northern part of district Peshawar, Pakistan. *Nat. Hazards* **2020**, *101*, 385–408. [CrossRef]

36. Roy, B.; Khan, M.S.M.; Islam, A.K.M.S.; Khan, M.J.U.; Mohammed, K. Integrated flood risk assessment of the Arial Khan River under changing climate using IPCC AR5 risk framework. *J. Water Clim. Chang.* **2021**, *12*, 3421–3447. [CrossRef]

37. Sharma, J.; Ravindranath, N.H. Applying IPCC 2014 framework for hazard-specific vulnerability assessment under climate change. *Environ. Res. Commun.* **2019**, *1*, 051004. [CrossRef]

38. Mustapha, A.; Yakudima, I.I.; Alhaji, M.; Nabegu, A.B.; Dakata, G.A.F.; Umar, A.Y.; Musa, U.B. Overview of the physical and human setting of Kano Region, Nigeria. *J. Geogr.* **2014**, *1*, 1–12.

39. Mohammed, A.; Dan'azumi, S.; Modibbo, A.A.; Adamu, A.A.; Ibrahim, Y. Rainfall-runoff modeling for Challawa and Jakara Catchment Areas of Kano City, Nigeria. *Arid. Zone J. Eng. Technol. Environ.* **2021**, *17*, 439–452.

40. Choubin, B.; Hosseini, F.S.; Rahmati, O.; Youshanloei, M.M. A step toward considering the return period in flood spatial modeling. *Nat. Hazards* **2023**, *115*, 431–460. [CrossRef]

41. Taromideh, F.; Fazloula, R.; Choubin, B.; Emadi, A.; Berndtsson, R. Urban Flood-Risk Assessment: Integration of Decision-Making and Machine Learning. *Sustainability* **2022**, *14*, 4483. [CrossRef]

42. Choubin, B.; Jaafari, A.; Henareh, J.; Hosseini, F.S.; Mosavi, A. Averaged Neural Network Integrated with Recursive Feature Elimination for Flood Hazard Assessment. In Proceedings of the IEEE 17th International Symposium on Applied Computational Intelligence and Informatics (SACI), Timisoara, Romania, 23–26 May 2023; pp. 000733–000738. [CrossRef]

43. Costache, R.; Pham, Q.B.; Sharifi, E.; Linh, N.T.T.; Abba, S.I.; Vojtek, M.; Vojteková, J.; Nhi, P.T.T.; Khoi, D.N. Flash-Flood Susceptibility Assessment Using Multi-Criteria Decision Making and Machine Learning Supported by Remote Sensing and GIS Techniques. *Remote Sens.* **2020**, *12*, 106. [CrossRef]

44. Wang, Y.; Hong, H.; Chen, W.; Li, S.; Pamučar, D.; Gigović, L.; Drobnjak, S.; Tien Bui, D.; Duan, H. A Hybrid GIS Multi-Criteria Decision-Making Method for Flood Susceptibility Mapping at Shangyou, China. *Remote Sens.* **2019**, *11*, 62. [CrossRef]

45. Efraimidou, E.; Spiliotis, M. A GIS-Based Flood Risk Assessment Using the Decision-Making Trial and Evaluation Laboratory Approach at a Regional Scale. *Environ. Process.* **2024**, *11*, 9. [CrossRef]

46. Dahri, N.; Yousfi, R.; Bouamrane, A.; Abida, H.; Pham, Q.B.; Derdous, O. Comparison of analytic network process and artificial neural network models for flash flood susceptibility assessment. *J. Afr. Earth Sci.* **2022**, *193*, 104576. [CrossRef]

47. Daffi, R.E.; Otun, J.A.; Ismail, A. Flood hazard assessment of River Dep Floodplains in North-Central Nigeria. *Intern. J. Water Res. Environ. Eng.* **2014**, *6*, 67–72.

48. Daffi, R.E.; Ismail, A.; Egharevba, N.S. Use of geographic information system techniques for flood inundation mapping of low-lying areas of River Dep Basin. *Niger. J. Trop. Eng.* **2015**, *8*, 1–8.

49. Cançado, V.; Brasil, L.; Nascimento, N.; Guerra, A. Flood risk assessment in an urban area: Measuring hazard and vulnerability. In Proceedings of the 11th International Conference on Urban Drainage, Edinburgh, Scotland, UK, 31 August–5 September 2008.

50. Olasunkanmi, A.B.; Dan'azumi, S. Flood inundation and hazard mapping of River Zungur Watershed using GIS and HEC-RAS Models. *Niger. J. Technol.* **2018**, *37*, 1162–1167. [CrossRef]

51. Birkmann, J. Framing vulnerability, risk and societal responses, the MOVE framework. *Nat. Hazards* **2013**, *67*, 193–211. [CrossRef]

52. Iyengar, N.S.; Sudarshan, P. A Method of Classifying Regions from Multivariate Data. *Econ. Political Wkly.* **1982**, *17*, 2047–2052.

53. Karmaoui, A.; Balica, S.F.; Messouli, M. Analysis of applicability of flood vulnerability index in Pre-Saharan region, a pilot study to assess flood in Southern Morocco. *Nat. Hazards Earth Syst. Sci. Discuss.* **2016**, *96*, 1–24. [CrossRef]

54. Sharma, S.V.; Roy, P.S.; Chakravarthi, V.; Rao, S.G. Flood risk assessment using multi-criteria analysis: A case study from Kopili River Basin, Assam, India. *J. Geomat. Nat. Hazards Risk* **2018**, *9*, 79–93.

55. Mukhtar, I. Analysis of Flood Risk and Vulnerability in Kano Metropolis, Kano State, Nigeria. Ph.D. Thesis, Department of Geography, Ahmadu Bello University, Zaria, Nigeria, 2018.

56. Houston, D.; Werritty, A.; Bassett, D.; Geddes, A.; Hoolachan, A.; McMillan, M. *Pluvial (Rain-Related) Flooding in Urban Areas: The Invisible Hazard*; Joseph Rowntree Foundation: Bristol, UK, 2011.

57. Lisetskii, F.N.; Buryak, Z.A. Runoff of Water and Its Quality under the Combined Impact of Agricultural Activities and Urban Development in a Small River Basin. *Water* **2023**, *15*, 2443. [CrossRef]

58. Nasidi, N.A. *Urbanism and the Conservation of The Natural Environment for Sustainable Development: A Case Study of Kano State, Nigeria, 1989–2020*; [Research Report] IFRA-Nigeria Working Papers Series 87; IFRA-Nigeria: Ibadan, Nigeria, 2022; pp. 1–20.

59. Cook, L.M.; McGinnis, S.; Samaras, C. The effect of modeling choices on updating intensity-duration-frequency curves and stormwater infrastructure designs for climate change. *Clim. Chang.* **2020**, *159*, 289–308. [CrossRef]

60. WMO (World Meteorological Organization); GWP (Global Water Partnership). *Integrated Flood Management Tools Series No. 20*; WMO & GWP: Zurich, Switzerland, 2013.

61. Khan, D.M.; Veerbeek, W.; Chen, A.S.; Hammond, M.J.; Islam, F.; Pervin, I.; Djoidjevic, S.; Buttler, D. Back to the Future: Assessing Damage of 2004 Dhaka Flood in the 2050 Urban Environment. *J. Flood Risk Manag.* **2016**, *11*, S43–S54. [CrossRef]

62. Rosmadi, H.S.; Ahmed, M.F.; Mokhtar, M.B.; Lim, C.K. Reviewing Challenges of Flood Risk Management in Malaysia. *Water* **2023**, *15*, 2390. [CrossRef]